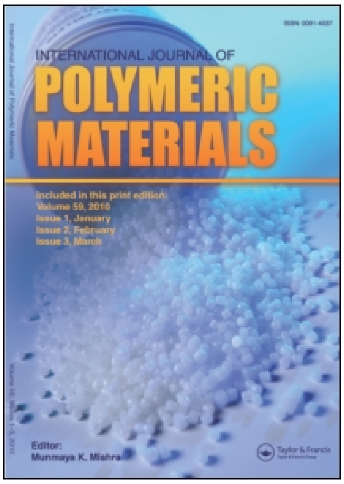

International Journal of Polymeric Materials
Publication details, including instructions for authors and subscription information:
http://www.informaworld.com/smpp/title~content=t713647664

On the Effect of Fiber Shape and Packing Array on Elastic Properties of Fiber-Polymer-Matrix Composites

Daining Fang[a]; Tieqi Liu[a]
[a] Department of Engineering Mechanics, Tsinghuta University, Beijing, China

To cite this Article Fang, Daining and Liu, Tieqi(1996) 'On the Effect of Fiber Shape and Packing Array on Elastic Properties of Fiber-Polymer-Matrix Composites', International Journal of Polymeric Materials, 34: 2, 75 — 90
To link to this Article: DOI: 10.1080/00914039608031467
URL: http://dx.doi.org/10.1080/00914039608031467

Intern. J. Polymeric Mater., 1996, Vol. 34, pp. 75–90
Reprints available directly from the publisher
Photocopying permitted by license only

On the Effect of Fiber Shape and Packing Array on Elastic Properties of Fiber-Polymer-Matrix Composites

DAINING FANG and TIEQI LIU

Department of Engineering Mechanics,
Tsinghuta University, Beijing 100084, China

(Received 23 March 1996)

In this study, three-dimensional finite element simulations on the base of the cell model and micromechanics are made to predict effective elastic properties of fibrous composites. The effects of fiber shape, packing array and volume fraction on the overall elastic behavior of an epoxy resin containing unidirectional glass fibers are examined. The geometrical structure includes three types of periodic fiber arrangements in cubic, hexagonal and rectangular cells. The fibers are assumed to be of four shapes; square, circular, elliptic and rectangular. The numerical results indicate that the overall transverse elastic properties are rather sensitive to both fiber shape and packing array while fiber geometry has no effect on the apparent overall Young's modulus in the longitudinal direction of the fibrous composite.

Keywords: Fibrous composite; elastic properties; finite element analysis.

1. INTRODUCTION

Continuously reinforced fibrous composites provide appealing possibilities for developing better specific stiffness and lighter weight than conventional metals and alloys. The overall behaviors of the fibrous composites are normally anisotropic, i.e., stress-strain relations depend on orientation even though the component materials may be isotropic. The determination of overall properties of the anisotropic fibrous composite has been the subject of considerable analytical and experimental research over the past several decades. Recently, the finite element method is getting increasing attention for modeling the overall properties of various composites [1–10]. The need for numerical analysis arise because of three major reasons: (1) analytical formulations become intractable, especially for nonproportional loading and in situation where the reinforcement phase contains shape corners [1], (2) micromechanical information cannot be extracted from experiments alone in a systematic manner [3], (3) the numerical method can be employed for the optimization design of the composite materials. For example, a possible method for improving composite properties may be to use non-circular fiber and to design specific packing arrangement for given application of the composites. Most of the reported work related to the numerical modeling was concerned with two-dimensional or axisymmetric cell models [2–6, 8–10] and with circular fibers or particle [2–10] due to the computational cost [1–3]. However, to numerically determine all of nine elastic constants of the orthotropic fibrous composites and to accurately examine the effect of fiber geometry on the overall mechanical properties, the three dimensional (3-D) analysis is necessary. In this investigation, overall elastic properties of epoxy resin-matrix composites reinforced with circular and non-circular glass continuous fibers are determined by 3-D finite element method in conjunction with cell models and micromechanics. The effect of fiber packing array and shape on the effective moduli is the principal concern of this paper. It is assumed that the fibers are arranged in three types of infinite periodic packing arrays, such as cubic, hexagonal and rectangular arrays. An attempt is made to assess the potential benefits to be gained from using non-circular fibers. The fiber shapes in the modeling, therefore, are taken to be cubic, circular, elliptic and rectangular. A description of material models with specific geometrical designs and the computational approach is given in Section 2. In Section 3, the numerical results are presented. Discussion and concluding marks are made in Section 4.

2. MATERIAL MODELS AND COMPUTATIONAL APPROACH

A fiber composite is modeled as a ductile matrix filled with unidirectional long fibers. Three uniform periodic arrays, such as cubic array, hexagonal array and rectangular array, lead to three types of fiber packing, as shown in Figure 1. The dash lines in Figure 1 constitute periodic cells. Each cell contains a fiber. Assumptions concerning the manner in which the fibers are distributed affect how fiber volume fraction is calculated. If the fiber is taken to be a cylinder with radius r, for example, the fiber volume fraction f can be calculated as

$$f = \lambda.(r/R)^2 \quad (1)$$

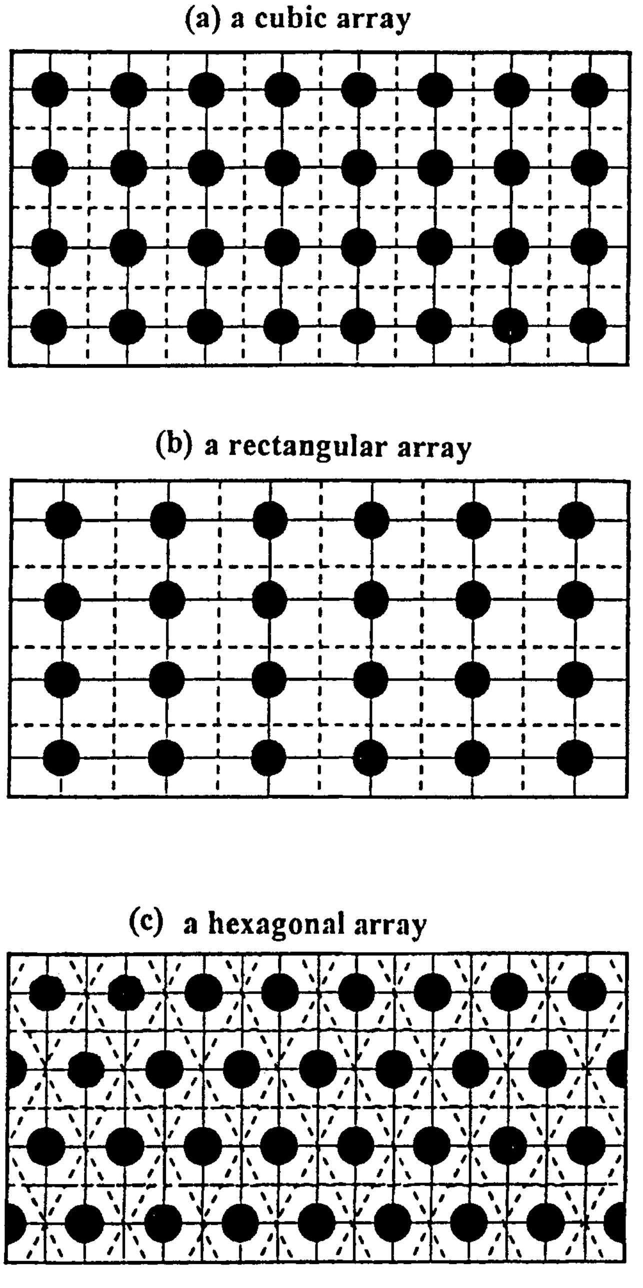

FIGURE 1 Schematic of periodic particle packing and cell array. (a) a cubic array, (b) a rectangular array, (c) a hexagonal array.

For the cubic array, $2R$ is the length of the side of the cubic cell, $\lambda = \pi/4$; for the hexagonal array, R is the length of the side of the hexagon, $\lambda = 2\sqrt{3}\pi/9$; and for the rectangular array, the λ is dependent on the ratio of lengths between two sides of the rectangular cell. In order to examine the shape effect of fibers on the elastic deformation, four shapes, such as cubic, circular, elliptic and rectangular parallelepiped, are considered, as shown in Figure 2. The fibers are aligned along the x_3-axis and Figure 2 shows fiber shapes on the transverse plane. To explain the effect of fiber geometry, the transverse fiber aspect ratio β_f and transverse cell aspect ratio β_c for a given loading-direction are specified, respectively,

$$\beta_f = l/w, \quad \beta_c = L/W \tag{2}$$

where w is the fiber width normal to the loading-direction and the length along a given loading-dirction on the transverse plane. For example, for the rectangular fiber subjected to x_1-direction loading, $w = b$ and $l = a$, and for x_2-direction loading, $w = a$ and $l = b$, as shown in Figure 2. For the circular fiber, $a = b = r$ and for the elliptic fiber, a, b are the length of minor axis and major axis. Similarly, W, L are the width and length of the cell for a given loading-direction on the transverse plane, respectively.

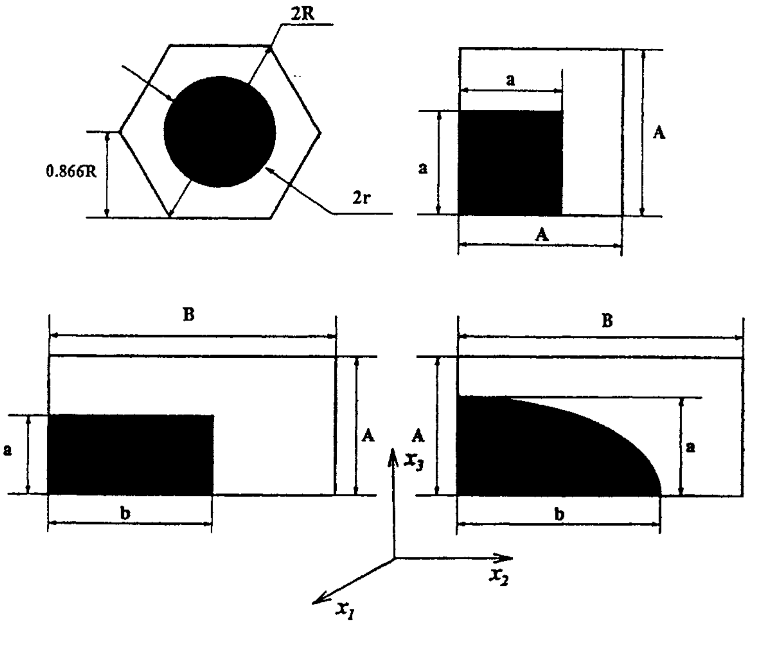

FIGURE 2 Schematic of four fiber shapes on the transverse plane.

The simulations in this paper were based on a three-dimensional (3-D) cell model of periodic fiber distributions, as shown in Figure 3. The elastic and compliance tensors, C and S, are periodic functions of the position. The periodic solutions can be expressed as

$$\sigma(x) = \sigma(x + \boldsymbol{d}), \quad \varepsilon(x) = \varepsilon(x + \boldsymbol{d}) \tag{3}$$

where

$$\boldsymbol{d} = \sum_{i=1}^{3} 2 m_i a_i \boldsymbol{e}_i \tag{4}$$

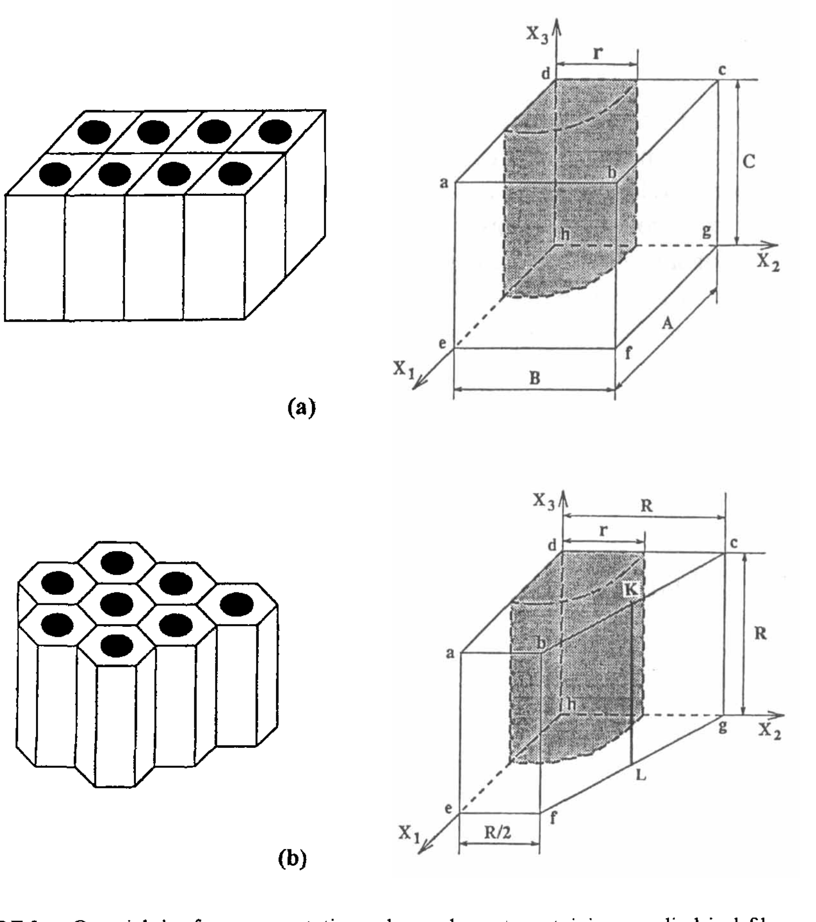

FIGURE 3 One-eighth of a representative volume element containing a cylindrical fiber: (a) the cubic or rectangular cell, (b) the hexagonal cell.

with $m_i = (i = 1,2,3)$ arbitrary integers, and $\boldsymbol{a}(= a_i \boldsymbol{e}_i)$ denotes the tensor of the unit cell edges. The average strain denoted by $\langle \varepsilon \rangle$, and the average stress denoted by $\langle \sigma \rangle$, are given, respectively, in terms of the prescribed boundary displacement $(\boldsymbol{u}^{\circ})$ condition by

$$\langle \varepsilon \rangle = \frac{1}{V}\int_{v} \varepsilon(x)\, dV = \frac{1}{V}\int_{\partial v} \frac{1}{2}(\boldsymbol{n}.\boldsymbol{u}^{\circ} + \boldsymbol{u}^{\circ}.\boldsymbol{n})\, ds \tag{5}$$

$$\langle \sigma \rangle = \frac{1}{V}\int_{v} \sigma(x)\, dV = \frac{1}{V}\int_{v} C(x) : \varepsilon(x)\, dV \tag{6}$$

The fibers are taken to be elastic and the matrix material is taken to be perfectly bonded to the fibers. The effective elastic moduli can be extracted from the relations

$$\langle \sigma \rangle = \boldsymbol{C}^{*}{:}\langle \varepsilon \rangle, \quad \langle \varepsilon \rangle = \boldsymbol{S}^{*}{:}\langle \sigma \rangle \tag{7}$$

Where $\boldsymbol{C}^{*}$ and $\boldsymbol{S}^{*}$ are the overall elasticity tensor and compliance tensor, respectively. For the purpose of convenient computation, it is often to express the stress-strain relation Eq. (7) in terms of a six-dimensional matrix. To this end, the overall compliance tensor $\boldsymbol{S}^{*}$ is represented by six by six matrix. Therefore, for an orthotropic composite material in which there are nine independent effective material constants, the effective compliance matrix in terms of effective engineering elastic constants is

$$[S_{ij}^{*}] = \begin{bmatrix} \frac{1}{E_{11}^{*}} & -\frac{v_{21}^{*}}{E_{22}^{*}} & -\frac{v_{31}^{*}}{E_{33}^{*}} & 0 & 0 & 0 \\ & \frac{1}{E_{22}^{*}} & -\frac{v_{32}^{*}}{E_{33}^{*}} & 0 & 0 & 0 \\ & & \frac{1}{E_{33}^{*}} & 0 & 0 & 0 \\ \mathit{Symm.} & & & \frac{1}{G_{23}^{*}} & 0 & 0 \\ & & & & \frac{1}{G_{13}^{*}} & 0 \\ & & & & & \frac{1}{G_{12}^{*}} \end{bmatrix} \tag{8}$$

where E is the Young's modulus, v is the Poisson's ratio, G is the shear modulus.

The finite element method has been used to solve the boundary value problems for the 3-D cell. For the prescribed boundary displacement $u^{\circ}|_{\partial V} = \varepsilon^{\circ}.x$, the overall elastic properties represented in sequel were computed using above constitutive formulas. The boundary conditions of a representative element must let the unit cell satisfy with the continuum condition and the periodic condition. Since the corresponding faces of a 3-D cubic cell or a 3-D rectangular cell are parallel (see Fig. 3a), the boundary conditions can be as simple as the outer faces of the unit cell are constrained to deform parallel and to remain planar with zero shear traction during deformation. For the 3-D hexagonal cell, the boundary conditions are more complicated than those of the cubic cell. As a result of symmetry, one-eighth of the hexagonal cell with a circular fiber is modeled, as shown in Figure 3b. Herein, the boundary conditions for a hexagonal cell loaded in tension are given as: (i) the interior planes of the cell are symmetric planes which can be restrained from moving in a perpendicular direction, (ii) the displacements within two outer planes, face (*abed*) and face (*abfe*), parallel to the symmetric planes, are constrained to move parallel; that is, the two outer planes of the cell are constrained to remain planar during deformation, (iii) the displacements u_1, u_2 (along the x_1, x_2 -direction) within the inclined plane, face (*bcgf*) of the cell, is constrained to be antisymmetric to the middle line KL of the face; that is, the inclined plane is constrained to remain an inclined plane, but only rotate along the middle line KL.

3. RESULTS

In this section, the numerical results of effective elastic moduli of fibrous composites are presented. To examine the effect of fiber geometrical parameters on the elastic deformation response of the composites, three cell array and periodic distributions of fibers are selected, as shown in Figure 1. In addition, four fiber shapes are considered, including cylindrical, elliptic, cubic and rectangular parallelepiped (see Fig. 2). Calculations are also made with varying fiber volume fraction. The material composes of an epoxy resin matrix which contains continuous glass fibers. The elastic properties of the matrix are $E_m = 3.42$ GPa and $v_m = 0.34$; for the particle, $E_f = 69.0$ GPa and $v_f = 0.2$. In all cases, there are two types of loading, that is, monotonic tensile loading and shear loading. A total of nine separate simulations are required to predict the effective elastic moduli. For the purpose of saving paper space, only effective axial and shear moduli to bring to light the key aspects of fiber packing and shape effects on the elastic behavior. The simulations correspond to the

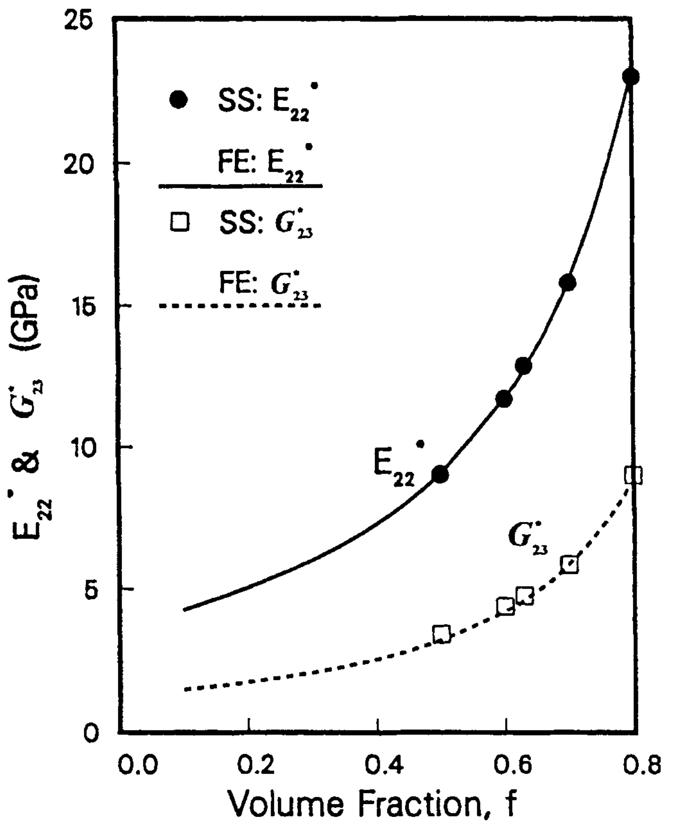

FIGURE 4 Comparison of E_{22}^* and G_{23}^* calculated from a series solution[11] and from the finite element method.

coordinates, x_1, x_2, x_3, in Figure 3. where the fibers are aligned with the x_3-direction.

Before applying the 3-D finite element method to examine the effect of the composite microstructure on the elastic properties, the cell model is employed to determine the effective moduli and to demonstrate its accuracy. The problem considered is that of a unidirectional fibrous glass/epoxy composite [11]. In that study, a series solution for the Airy stress functions and displacements was determined. For a hexagonal array with a volume fraction $f = 0.6$, the effective axial Young's modulus was found to be 42.82 *GPa* by the Pickett [11]. In this work, in terms of the finite element method, we got $E_{33}^* = 42.825$ *GPa*, the difference is about 0.01%. Again in the reference [11] a unidirectional fibrous glass/epoxy composite was considered. In this case, a

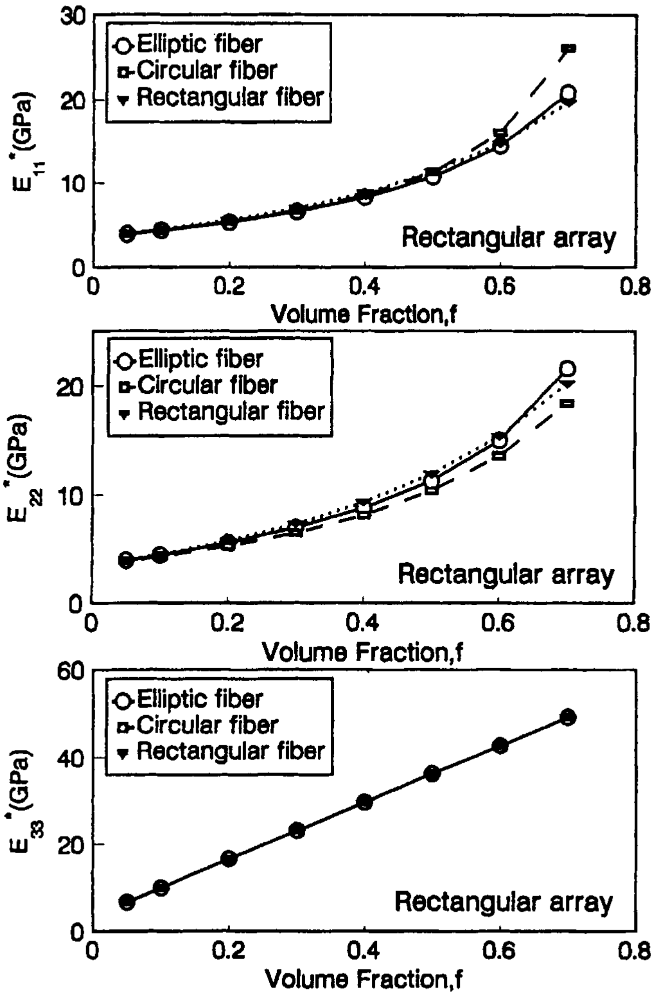

FIGURE 5 Effect of fiber shape for the rectangular array on effective Young's moduli.

rectangular fiber array was chosen with a volume fraction $f = 0.6$. The effective moduli, E_{22}^* and G_{23}^*, calculated by the series solution and by the 3-D finite element method, are illustrated in Figure 4 where there is rather small difference between two sets of the results. When the volume fraction is larger than 60 percent, the elastic moduli increase significantly.

In order to examine the combined effect of fiber shape and packing array on the composite properties, two modeling cases are considered in the numerical analysis. One is the rectangular packing array with transverse cell aspect

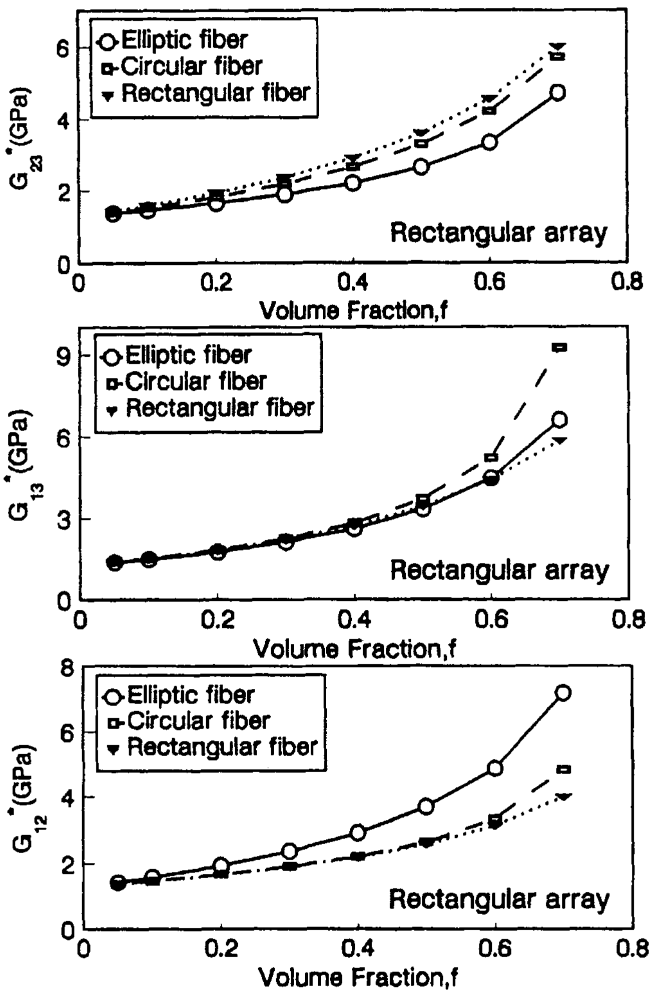

FIGURE 6 Effect of fiber shape for the rectangular array on effective shear moduli.

ration $\beta_c = 0.577$ for loading in the x_1-direction and 1.733 for loading in the x_2-direction. In this case, there are three fiber shapes, including the elliptic, rectangular and circular whose transverse fiber aspect ratio β_f is equal to 0.577, 0.667 and 1.0 for loading in the x_1-direction and 1.733, 1.5, 1.0 for loading in the x_2-direction, respectively. Another case is the cubic array ($\beta_c = 1.0$ for any directions) with the cubic, circular and rectangular fibers which have $\beta_f = 1.0$, 1.0 and 0.667 for loading in the x_1-direction and 1.0, 1.0 and 1.5 for loading in the $x_2$direction. In two cases, the fiber volume fraction varies from 5 to 70 percent. Results of the effective axial and shear module for the first case are presented in Figure 5 and Figure 6. For all two kinds of fiber shapes and cell arrays, increasing the volume fraction results in a stiffer macroscopic response for the composites. That is, the reinforcing effect of the fibers leads to enhanced stiffness and the macroscopic composite stress is greater than the stress in the unreinforced matrix case at all load levels. On the other hand, it can be found from Figure 5 that the three overall axial moduli for a fixed volume fraction are different and the enhancement in the fiber longitudinal direction is far larger than in the transverse directions, which does reflect the anisotropic constitutive response. Figure 5 shows the effective Young's modulus, E_{33}^*, along the direction of fiber alignment is independent on the fiber shapes. In case that the composite is subjected to transverse tension, the shape effect on the moduli increases with the increase of the volume fraction. The greatest differences of E_{11}^*, E_{22}^* for three shapes at the volume fraction of 70 percent are 24.45% and 14.81%, respectively. For E_{11}^*, the reason that the circular fiber leads to the largest stiffness is due to its higher transverse fiber aspect ratio $\beta_f(=1.0)$ in x_1-direction at a fixed volume fraction. Similarly, because the $\beta_f(=1.733, 1.5)$ of the elliptic or rectangular fiber in x_2-direction is larger than that $(=1.0)$ of the circular fiber, the E_{22}^* of the composite with the circular fiber is obviously higher. In comparing Figure 5 and Figure 6, it is clear that the effect of the fiber shape on the shear moduli is larger than on the axial Young's moduli. For example, the greatest difference of G_{23}^*, G_{13}^* and G_{12}^* at $f = 0.7$ for three shapes are 21.1%, 40.34% and 44.36%, respectively. Figure 6 indicates that each shape gets one of the largest shear moduli and other two shapes' results are very closed. For the rectangular array, it is difficult to explain the effect of fiber shapes on the effective shear moduli by means of either transverse fiber aspect ratio or cell aspect ratio because the effect of fiber shape and packing array is combined during the shear loading imposed on two directions of the rectangular cell faces. Therefore, for the purpose of accounting for the shape effect on the shear moduli, the second case was considered. In this case, the transverse cell aspect ratio for any direction equals to 1.0, thus the transverse fiber aspect ratio is one key factor which reflects the shape influence. Results for this case are demonstrated in Figure 7. For the rectangular fiber, its β_f is larger in x_2-direction and smaller in x_1-direction than that for the cubic and circular fibers, which results in the largest G_{23}^* and the smallest G_{13}^* in comparing with the results of the cubic and circular fibers, as shown in Figure 7. The nearly same values of the G_{23}^* and G_{13}^* between the cubic and circular fibers are due also to their same $\beta_f(=1.0)$. However, it is found from Figure 7 that the effective shear moduli G_{12}^* is almost independent of the fiber shapes for the cubic array. Comparing Figure 6 with

Figure 7, we may know that the G_{12}^* for the rectangular packing array is related not only to the fiber shape, but to the fiber packing array.

The next problem considered is the effect of fiber packing on the overall elastic behavior. A cylindrical fiber is aligned in terms of three types of the perfect periodic packing arrays which includes the hexagonal, rectangular and cubic. The numerical predictions for the effective Young's moduli are exhibited in Figure 8 for three types of the arrays. Again, a different trend is found between longitudinal tension and transverse loading. It is clear while Young's

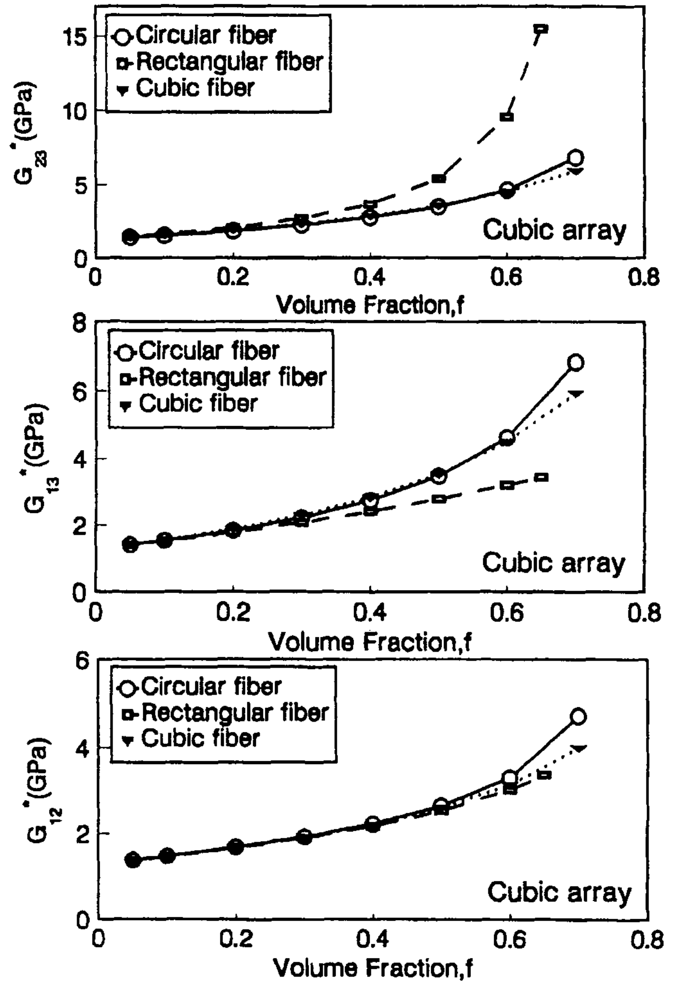

FIGURE 7 Effect of fiber shape for the cubic array on effective shear moduli.

modulus, E_{33}^*, is essentially independent of fiber packing arrangement, the effective Young's moduli in the transverse direction are affected by the fiber packing array. This geometry dependence, which is negligible for axial deformation, becomes significant when the volume fraction increases. The greatest differences of E_{11}^* and E_{22}^* at $f = 0.7$ are 39.18% and 24.91%, respectively. On the transverse tension, the effect of the fiber packing arraignment on the elastic moduli seems relative to the transverse cell aspect ratio in a given loading direction. For example it can be seen from Figure 2 and Equation (2) that the β_c

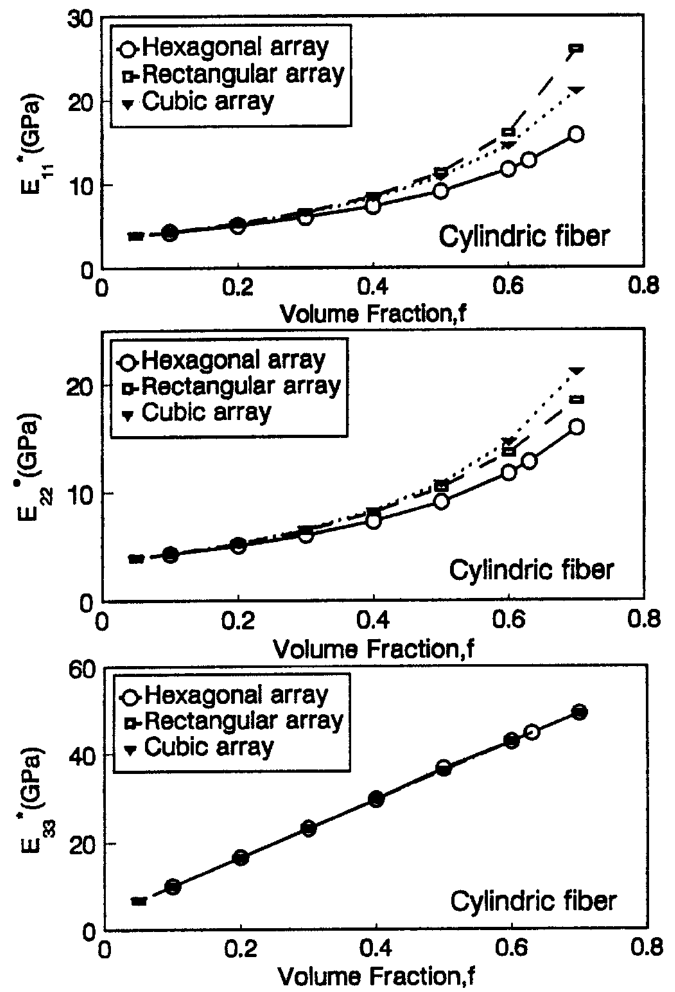

FIGURE 8 Effect of fiber packing array for the cylindrical fiber on effective Young's moduli.

of the rectangular array for the x_1-direction of 0.577 which is smaller than that of the cubic array or hexagonal array. Thus, its E_{11}^* is larger in comparison to that of the cubic array or hexagonal array. Also shown in Figure 8 is that E_{11}^* for the cubic and hexagonal arrays is equal to E_{22}^*, which does reflect the square symmetry of the cubic array and the transverse isotropic properties of the hexagonal array on the transverse plane. Similarly, the smallest $\beta_c(=1.0)$ of the cubic array in x_2-direction in comparing with the hexagonal and rectangular packing arrays leads to the largest E_{22}^* and the strongest enhancement in x_2-direction. Tvergaard [2] has illustrated that the stress-strain curve of the fiber composites is dependent on the cell aspect ratio. i.e. on fiber spacing. That is, the influence of fiber distributions reflects the effect of fiber spacing for a given fiber shape.

4. DISCUSSION AND CONCLUSIONS

The elastic constitutive properties and overall moduli of the epoxy resin-matrix fibrous composites subjected to tension and shear loading have been examined numerically. The results reveal that the microstructure of the composite has a decisive effect on the overall transverse properties of the fibrous composites. Therefore, optimization of the overall mechanical properties of the fibrous composite thorough the manipulation of its geometrical structure inevitably requires a thorough understanding of fiber geometry and distribution effects. The sensitivity of the overall transverse moduli to changes of various geometrical parameters has been evaluated by a number of computations demonstrated in Figure 5 ~ Figure 8. Some conclusions can be obtained from the numerical results as follows:

1. Results exhibited in Figure 5 and Figure 7 show the axial Young's modulus of the composite is essentially insensitive to either the fiber shape or packing arrangement.

2. Two geometrical factors, fiber shape and packing, do affect the transverse properties. The effect of the fiber packing array actually represents the influence of the transverse cell aspect ratio. The smaller the transverse cell aspect ratio in a given direction for a given fiber shape, the larger the transverse Young's moduli for the given direction.

3. The effect of fiber shape on the overall elastic properties is dependent on the transverse fiber aspect ratio. Varying the transverse fiber aspect ratio have a somewhat larger effect, as shown in Figure 5–Figure 8, and changes of the fiber volume fraction has quite a strong influence. In other words, the different fiber shapes lead to different values of the transverse fiber aspect ratio which in

fact affect the elastic properties of the composites. It may conclude that for fixed values of all other material parameters, the larger the transverse fiber aspect ratio for a given direction, the higher the effective transverse Young's moduli and shear moduli in that direction of the ductile matrix composites reinforced with brittle fibers.

4. The effect of the fiber shape on the shear moduli is stronger than on the transverse Young's moduli, especially when the volume fraction becomes large.

5. The effect of fiber shape and packing array on the elastic properties of the composite becomes significant with the increase of the fiber volume fraction.

According to above conclusions, we believe that in addition to obtaining detailed stress and strain fields on the order of fiber diameter to accounting for stress-strain relation of composite materials, the numerical method has an obvious advantage of characterizing the fiber geometry, thus, accounting for geometrical influence of fibers on the mechanical properties. The results indicate that the local properties become stress-dependent and the overall elastic constitutive response of composites is influenced by the distribution and shape of the continuous fibers. In general, the higher a transverse fiber aspect ratio or the smaller a transverse cell aspect ratio in a given direction of a composite, the more effective reinforcement in that direction. However, the present analyses are based on the idealized assumptions of perfect periodic arrays and perfect bonding between the matrix and the fiber. According to experimental observation, the fibers are randomly distributed in general. A change of geometrical parameters leading to a higher stress level should usually result in a lower ductility. Therefore, further work should be focused on simulating and modeling the effect of fiber debonding and fiber random distribution on elastic and plastic properties.

Acknowledgments

Support from National Education Committee of China under grants for doing research at the [Solid Mechanics] Open Laboratory of Tongji University.

References

[1] Brockenbrough, J. R., Suresh, S. and Wienecke, H. A. (1991) *Acta Metall. Mater.*, **39**, 735–752.
[2] Tvergaard, V. (1990) *Acta. Metall. Mater.*, **38**, 185–194.
[3] Nakamura, T. and Suresh, S. (1993) *Acta Metall. Mater.*, **41**, 1665–1681.
[4] Guild, F. J. and Young, R. J. (1989) *J. Mater., Sci.*, **24**, 298–306.
[5] Needleman, A. and Tvergaard, V. (1993) *J. Appl. Mech.*, **60**, 70–76.
[6] Dorvak, G. J. and Bahei-El-Din, Y. A. (1982) *J. Appl. Mech.*, **49**, 327–325.
[7] Levy, A. and Papazian, J. M. (1990) *Metall. Trans. A.*, **24A**, 2487–2496.

[8] Bao, G., Hutchinson, J. W. and McMeeking, R. M. (1992) *Acta Metall. Mater.*, **40**, 2547–2555.
[9] Christman, T., Needleman, A. and Suresh, S. (1989) *Acta Metall.*, **7**, 3029–3050.
[10] Llorca, J. Needleman A. and Suresh, S. (1991) *Acta Metall.*, **39**, 2317–2335.
[11] Pickett, G. (1968) in Fundamental Aspects of Fiber Reinforced Plastic Composites, eds. R.T. Schwartz, Interscience Publishers, New York, 13–27.